The Foaming Window – A New Concept and Mechanism for Biocomposite Foams Processing by Two-Step Sintering

O. Gingu[1,*], G. Sima[1], C. Teisanu[1], C. Marinescu[2], A. Sofronia[2], S. Tanasescu[2] and P. Rotaru[1]

[1]*University of Craiova, 13 A.I. Cuza Street, 200585, Craiova, Romania*

[2]*Institute of Physical Chemistry Ilie Murgulescu of the Romanian Academy, 060021 Bucharest, Romania*

Abstract: The two steps sintering process provide economical, technological and innovative advantageous aspects to produce biocomposite foams for alloplastic bone grafts applications. The *kinetic window* mechanism, working during the 2nd TSS step, provides the nanostructured ceramic matrix, respectively improved biocompatibility. Simultaneously, the high porous structure, fitting the trabecular bone tissue, remained an important technical request of such applications up to this research. The porous biocomposite scaffold could be designed using specific foaming agents, like titanium hydride, calcium carbonate and ammonium bicarbonate, by controlling the foaming reactions depending on the foaming agents' type and content into the chemical composition of the initial biocomposite powder mixture. The new concept of *foaming window*, working during the 1st TSS step, includes these factors able to provide the specific foam structure fitting the required biocomposite foams porosity. Both windows may work for the benefit of the nanostructured highly porous biocomposite manufacturing by TSS process, in advantageous technical and economical terms.

Keywords: Biocomposite foams, two-steps sintering, nanostructure, foaming reactions.

1. INTRODUCTION

The two steps sintering (TSS) process is special recommended for the elaboration of highly dense (>98% ρ_t) nanostructured (20-200 nm grain size) ceramic materials, especially using a conventional furnace [1]. This outstanding achievement is due to the conventional sintering process divided in two steps: the 1st step manages the initiation of the diffusion process between the powder particles at a specific temperature ($T_{1\text{-}TSS}$) for short time ($T_{1\text{-}TSS}$, about some minutes) and the 2nd step by quick cooling down up to the next dwell temperature, $T_{2\text{-}TSS}$, when the densification process develops without grain growth, for even long times ($T_{2\text{-}TSS}$, about x10 hours range).

The progress of TSS process recorded the development of the *kinetic window* mechanism, occurring during the 2nd TSS step [2, 3]. The correlation between the grain boundary diffusion and grain boundary migration creates this *kinetic window* which allows the elaboration of full dense nanostructured ceramics. Outside the *kinetic window*, depending on the relationship between the $T_{2\text{-}TSS}$ and $T_{2\text{-}TSS}$, full dense materials with grain growth or porous materials without grain growth may be elaborated [4].

Based on this *kinetic window*, advanced porous biocomposite materials with nanostructured ceramic matrix reinforced by micrometric metallic/ceramic particles were manufactured for potential alloplastic bone reconstruction applications [5-8]. The nanostructured hydroxyapatite matrix, which is assured by the TSS technology, respectively the *kinetic window*, represents a key-element for the biocompatibility enhancing, namely osteoblasts proliferation [9, 10]. On the other hand, the biocompatibility is related to the material porosity, the trabecular tissue being more porous (15-70%), with open and interconnected cells, than the cortical bone tissue (5-12% porosity) [11, 12].

This research proposes a new mechanism related to the TSS process, as a modern concept and instrument to design and elaborate the biocomposite materials for alloplastic bone grafts, with specific tailored porosity depending on the grafting placement. This concept is entitled *foaming window* and focuses on the foaming reactions designing and coordination in such a manner that the compact billet from biocomposite powder particles, including special foaming agents, will reach the required cellular structure during the 1st TSS step. The *foaming window* is strongly related to the *kinetic window* along the 2nd TSS step, which controls the development of the nanostructured ceramic matrix without nanometric hydroxyapatite grain growth.

2. MATERIALS AND METHODS

2.1. Biocomposite Foams Designing

The nanometric hydroxyapatite (HAP) powder particles (<200 nm; >99,99% purity; Sigma-Aldrich)

*Address correspondence to this author at the University of Craiova, 13 A.I. Cuza Street, 200585, Craiova, Romania; E-mail: oanagingu@yahoo.com

E-ISSN: 2409-5826/17 **© 2017 Avanti Publishers**

represent the biocomposite ceramic matrix. The titanium hydride (water atomised TiH_2; < 150 μm; Merck) works as reinforcement precursor for the TiO_2. In the same time, TiH_2 take part to the foaming reactions as well as calcium carbonate ($CaCO_3$, purity ≥ 99.0%, density 2.93 g/cm^3) powder particles and ammonium bicarbonate (NH_4HCO_3; purity ≥ 99.0%, density 1.58 g/cm^3, particle size of 250 μm...1.5 mm, irregular shape from Chimreactiv SRL, Bucharest, Romania) playing as blowing foaming agents role, Table **1**.

Table 1: Biocomposite Components and their Role for Material Designing

HAP (nm)	matrix	
TiH_2 (μm)	Reinforcement precursor	Foaming agents
$CaCO_3$ (μm) NH_4HCO_3 (μm)		

The biocomposite samples were designed as the Table **2** presents.

2.2. Biocomposite Foams Preparation

The HAP powders were calcinated in air at 900°C in air for 2 hours, using as heating rate 10°C/min. and cooling rate by furnace. The homogeneous mixture of HAP and TiH_2 was prepared by mechanical mixing in a Fristch Pulverisette 6 planetary ball mill. The 125 ml stainless steel vial was loaded in 2:1 ratio of milling balls (stainless steel, 5 mm diameter): powder mixture, using a wet milling environment (1 ml ethanol for 1 g of powder mixture). The mixing stage took 30 minute at 200 rpm and then the slurry was dried by night in the open door furnace heated at 100-150°C for alcohol removal. The dried slurry was mechanically mixed again in the ball mill for 5 minute in order to homogenize the powder mixture and then the milling balls were removed. The other foaming agents ($CaCO_3$ and NH_4HCO_3) were added to the powder mixture accordingly (see Table **2**).

Cylindrical billets (10 mm diameter; 5 mm height) were unilaterally cold compacted at 120 MPa and then sintered in argon atmosphere (99,99% purity) by the two-steps sintering (TSS) process, Figure **1**, the sintering parameters being presented in Table **3**. For all the sintering cycles, the samples were cooled down by furnace.

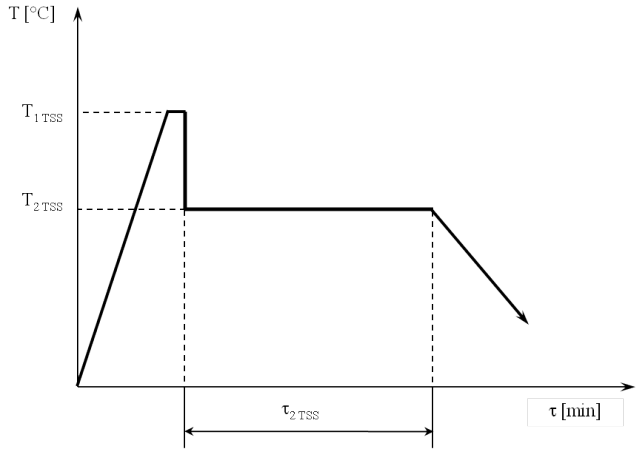

Figure 1: Schematic representation of TSS process.

Table 3: TSS Technological Parameters for Biocomposites Processing

TSS parameters			
1st Step heating Rate 10°C/min		2nd Step	
T_1 [°C]	T_1 [min]	T_2 [°C]	T_2 [min]
900	1-10	800	600

2.3. Biocomposites Foams Characterisation

The thermal analysis (TA) was performed for each biocomposite component in order to depict the critical temperatures for the foaming reactions (i.e., TiH_2, $CaCO_3$ and NH_4HCO_3), respectively for the self/diffusion reactions (i.e., HAP and HAP+TiH_2) as input data for the sintering process. A horizontal "Diamond Differential / Thermogravimetric Analyser"

Table 2: Chemical Composition of the Biocomposite Samples

Matrix, HAP [% wt]	Foaming agents [% wt.]		Sample code
75	25	TiH_2	BIO-1
		TiH_2 + NH_4HCO_3	BIO-2
		TiH_2 + $CaCO_3$	BIO-3
		TiH_2 + $CaCO_3$+ NH_4HCO_3	BIO-4

(Perkin elmer Instruments) was used for the TA carried out in dynamic argon atmosphere (150 cm^3 x min^{-1}) in non-isothermal linear regimes. Each biocomposite powder was heated in an alumina crucible in the temperature range (RT...1200)^{o}C. The heating rate was the same, 10C/min, for each heating cycle.

The optical inspection of the sintered samples was carried out by the stereomicroscope NIKON SMZ 745T equipped with imaging software NIS-A EDF and NIS-A AMEAS, respectively the optical metallographic inverted microscope Eclipse MA 100 (Nikon, Japan) equipped with NIS-Elements imaging software 3.0 and NIS-Elements BR.

The electronic microscopy analysis of the sintered biocomposite foams was performed by the Tescan Vega II–XMU equipment, maximum resolution 3,5 nm.

The biocomposite porosity was evaluated by means of the NOVA 2200e Quantachrome analyser, equipped with QuantachromeNovaWin©1994-2010 software, to determine the specific surface and pores volume using the Brunauer-Emmett-Teller (BET) method. Before the measurements, the samples were degassed for 6 hours at 150^{o}C in vacuum (10^{-2} Torr) to remove the water and gas traces.

3. RESULTS AND DISCUSSIONS

The experimental results focus on the effect of the foaming reactions during the 1st TSS step on the topography and porosity of the biocomposite samples, directly related to the foaming agent content of the biocomposite samples.

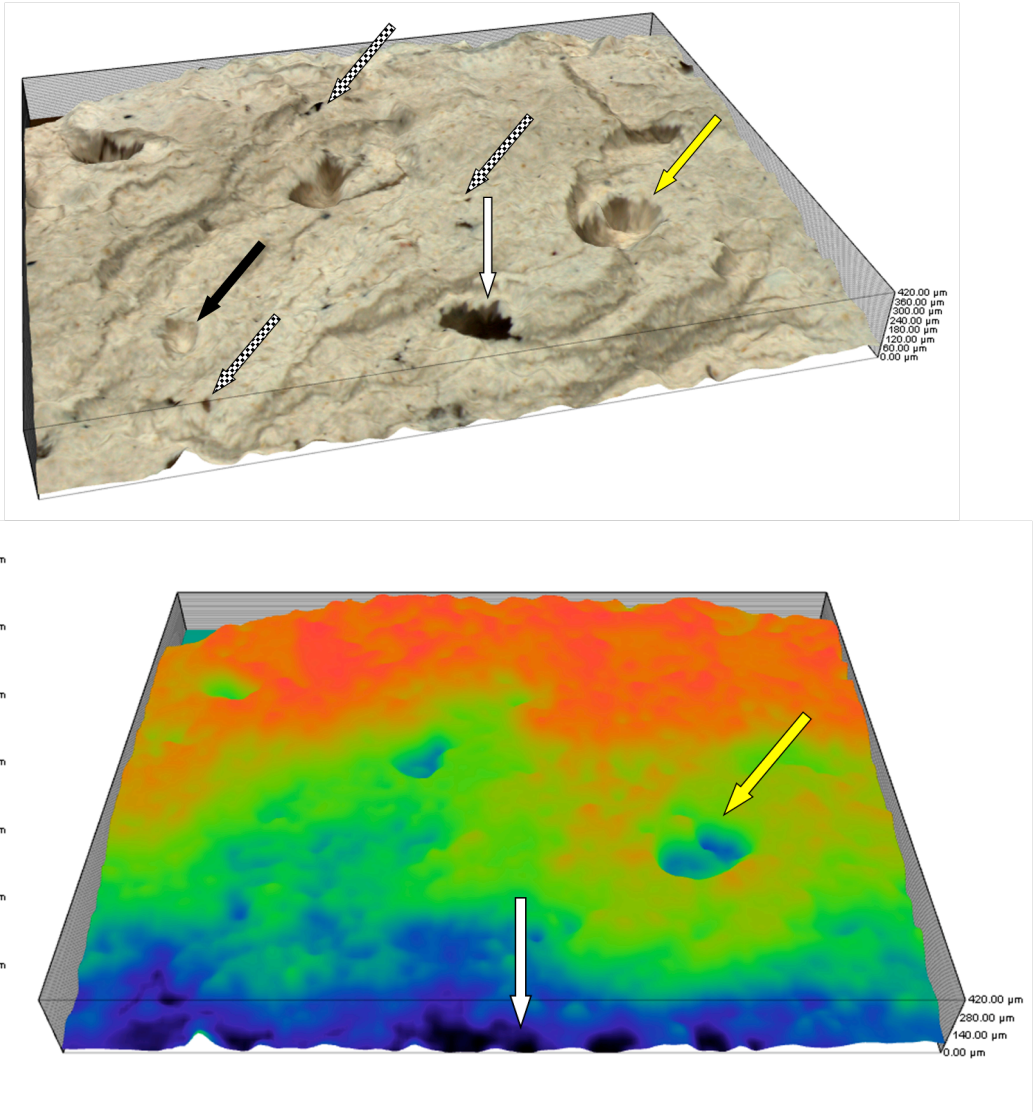

Figure 2: (**a**) Pore types of the BIO-3 samples (fractured surface), (**b**) Macroscopic topography of BIO-3 samples.

3.1. Thermal Analysis

The foaming reaction represents a complex process generated by successive chemical responses of the foaming agents during the biocomposites heating stage. The titanium hydride, ammonium bicarbonate and calcium bicarbonate used in our research take part from the blowing agents' category, successively generating gases or even vapours during their heating as individual foaming components [13-17]. Furthermore, the ammonium bicarbonate is especially recommended as blowing agent to increase the porosity level, with non-residual reaction products after sintering [18].

The presence of the hydroxyapatite, as the biocomposites matrix, determines significant changes of the foaming reactions kinetics during the materials' sintering [7, 18, 19]. The final structure of the processed biocomposites by TSS route presents nanostructured hydroxyapatite matrix reinforced by complex compounds of Ca and Ti-based [6, 7].

The foaming reactions create different kind of pores (size, volume and connectivity type) depending on the nature and content of the foaming agent. This phenomenon occurs along the 1st TSS step, during the heating stage from the RT to 900^{o}C. The biocomposite scaffold built by this mechanism reaches the dwell temperature $T_{1\text{-}TSS}$ (900^{o}C), corresponding to the initiation of diffusion reactions between the biocomposite components: nanometric HAP particles and Ti- and Ca-based compounds already synthesized during the TSS heating (1st step). The initiation of the diffusion reactions takes place during the $\tau_{1\text{-}TSS}$ dwell time (1-10 min.) at $T_{1\text{-}TSS}$ temperature (900^{o}C). The 2nd TSS step starts by the quick temperature decreasing up to $T_{2\text{-}TSS}$ level (800^{o}C) which blocks the grain growing and provides the nanostructured HAP sintered matrix at the end of the sintering process after $\tau_{2\text{-}TSS}$ dwell time (600 min.) [5].

3.2. Microscopical analysis

The optical inspection of the sintered biocomposites BIO-3 showed open (white arrow), closed (black arrow) and intercommunicated macropores (yellow arrow), Figure **2a**, **b**, beyond other types of pore (dotted arrows).

The macroscopically analysis underlines the roughness of the biocomposite samples (H_{max} = 420 μm) which corresponds to the trabecular bone characteristics as well as the open, closed and interconnected pores presence [20].

The scanning electron microscopy reveals a closure view on the foaming agents effect during the 1st TSS step for biocomposites processing. The comparative images on the BIO-1 (Figure **3a**) and BIO-4 (Figure **3b**) point out the role of the $CaCO_3$ and NH_4HCO_3 foaming reaction to produce larger pores (micrometric range) for BIO-4 series than for the BIO-1 series (with submicronic sized pores).

The experimental results presented above prove the significant influence of the $CaCO_3$ and NH_4HCO_3 addition to the TiH_2 component, by means of the pores' total volume and biocomposite porosity due to the phenomenon occurring during the 1st TSS step.

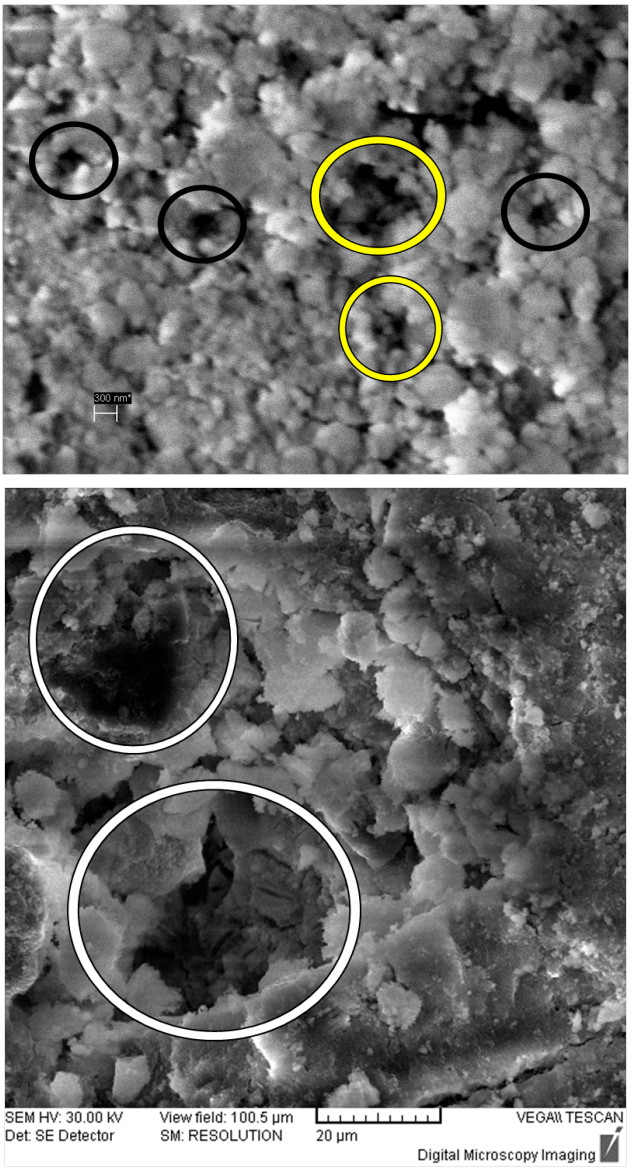

Figure 3: (**a**) SEM image on BIO-1 samples showing submicronic sized closed (black circles) and interconnected (yellow circles) pores (300 nm scale line), (**b**) SEM image on BIO-4 samples showing micrometric pore sized (white circles).

3.3. Porosity Evaluation

According to the experimental data reported on the HAP nanoparticles sintering, high density (>97% ρ_t, respectively 3% porosity) parts was obtained by TSS, respectively novel TSS route [21].

The addition of TiH_2 (BIO-1 samples) as precursor for TiO_2 plays an important role as ceramic reinforcement as well as blowing agent to increase the biocomposite porosity (average 30%) [22, 23]. The total volume of the pores measured by the BET method is 8,45...10,37 x $10^{-3}cm^3/g$ and the pore average radius is 1,73...1,91nm.

One of the most recommended blowing agents is the ammonium bicarbonate. The foaming reaction develops at low temperatures (40-130)$^{\circ}$C, depending on the powder mixture type, and all the foaming reaction products are volatile, generating bubbles [18, 24]. For our research, in order to raise the porosity level [18], the ammonium bicarbonate was added to TiH_2 (BIO-2 samples), and in that case the porosity reached 40% [5]. On the other hand, the addition of $CaCO_3$ to TiH_2 (BIO-3 samples) determined higher porosity level (max. 46%) than for BIO-2 samples [5]. We can assume that $CaCO_3$ provides a stronger foaming effect than the ammonium bicarbonate. Therefore we may connect this effect to the foaming temperatures for each blowing agent separately, as literature reports: 400-800^{0}C for TiH_2 [13], respectively 650-900°C for CaCO3 [16, 17].

As far as BIO-4 samples concerns, the obtained porosity is similar to BIO-2 samples (max. 40%), but the total volume of the pores is about 3 times higher than for BIO-1 samples whereas the pore radius is similar (1,69...1,89 nm). It would be assumed that the foaming effect generated by $CaCO_3$ is complementary to that provided by the ammonium bicarbonate by means of the pore number, respectively total volume (25,83...28,31 x $10^{-3}cm^3/g$).

Considering the foaming agents type, content, and foaming reactions along the 1st TSS step for biocomposites manufacturing, we may state a new mechanism in BIO samples designing entitled *foaming window*. This instrument could be connected to the kinetic window usually used for the nanostructured materials processed by TSS process, during its 2nd step [4]. The graphical representation of the *foaming window* is showed in Figure **4**.

The relevance of the *foaming window* mechanism is great because it is responsible for the biocomposite scaffold construction, respectively the porous structure, due to the complex foaming reactions occurring during the 1st TSS step, namely the heating stage. Once the

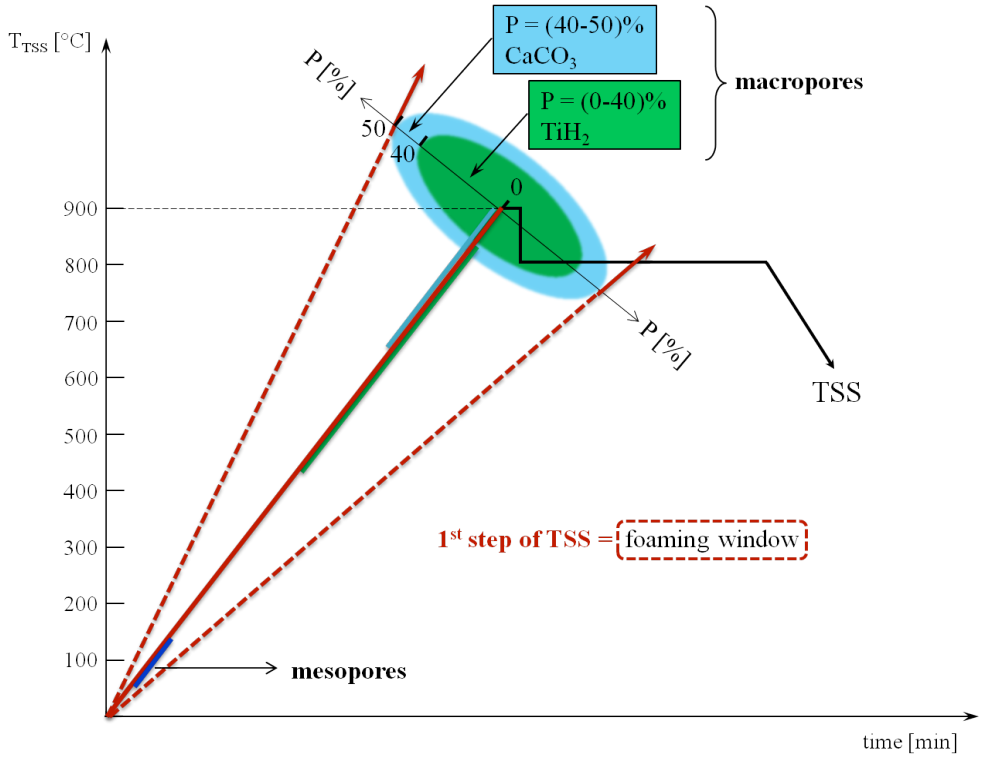

Figure 4: The foaming window mechanism related to the 1st TSS step to produce nanostructured biocomposite materials.

scaffold is built, the diffusion reactions between the biocomposite components develop, also during the 1st TSS step, but at the dwell temperature $T_{1\text{-}TSS}$, for short time (1-10 min.). The densification process takes place along the 2nd TSS step when the kinetic window has an important role on the final sintered nanostructure synthesis.

According to the Figure **4**, the 1st TSS step-heating stage (continuous red line) presents three foaming stages corresponding to the studied foaming agents. The main effect of the *foaming window* is evaluated by means of the porosity level [P%] of the processed biocomposite materials, and the "size" of this window (the cone delimited by the red dotted lines) depends on the foaming agent's content into the biocomposite chemical composition.

The mesopores of the biocomposite scaffold are attributed to the low temperature foaming agent generated by the ammonium bicarbonate. The high temperature foaming agents, respectively titanium hydride and calcium carbonate, lead to the macrospores' formation, but successively in this order, according to the foaming temperatures: TiH_2 has a great influence for lower porosity than 40% and $CaCO_3$ for higher, up to 50%. The porosity level presented in Figure **4** includes, also, the experimental data on microstructured biocomposites processed from micrometric HAP powder particles, which will be published in a future paper.

CONCLUSIONS

The *foaming window* mechanism is a new developed concept, based on the necessity to design the nanostructured biocomposites' scaffold since the 1st TSS step, during the heating stage. The foaming reactions, generated by the foaming agents, are responsible for the cellular structure of the biocomposite material. Depending on the alloplastic bone graft texture, namely cortical (dense) or trabecular (porous), the 1st TSS step must be monitored from the point of view of the type and content of the foaming agents incorporated into the initial powder mixture.

The following statements may be assumed concerning the blowing agents' role and effects:

- TiH_2 generates up to 25-27% porosity over that corresponding to the nanostructured HAP biomaterials. It would be the most significant contribution to produce biocomposite foams as alloplastic grafts for cortical/trabecular bone tissue;
- NH_4HCO_3 adds its contribution of about 10% porosity over the titanium hydride one. In the same time it may be assumed it is responsible of the mesopores formation since low temperatures of the 1st TSS step.
- $CaCO_3$ could give max. 15% porosity over the titanium hydride's contribution. Moreover, this blowing agent determines the increasing of the pores number, respectively total pore's volume, due to the foaming reaction occurring at high temperature, close to the end of the 1st TSS step.

The *foaming window*, acting in the 1st TSS step, is strongly related to the kinetic window which works in the 2nd TSS step, both mechanisms leading to the processing of nanostructured biocomposite materials with wide range of porosity level.

ACKNOWLEDGEMENTS

The authors are grateful to the research project PN-II-PT-PCCA-2013-4-2094, title: "*Research on the bone substitution with biocomposite materials processed by powder metallurgy specific techniques"* (acronym BONY) and the research group coordinated by Prof. Habil. Vasile Danut Cojocaru from the University Politehnica of Bucharest, Romania, for the SEM analysis.

REFERENCES

[1] Chen IW and Wang XH. Sintering dense nanocrystalline ceramics without final-stage grain growth. Nature 2000; 404:168-71. https://doi.org/10.1038/35004548

[2] Wang X, Deng X, Bai H, Zhou H, Qu W, Li L, *et al.* Two-step sintering of ceramics with constant grain-size, II: BaTiO3and Ni–Cu–Zn Ferrite, J Am Ceram Soc 2006; 89(2): 438-43. https://doi.org/10.1111/j.1551-2916.2005.00728.x

[3] Wright GJ and Yeomans JA. Constrained sintering of yttria-stabilized zirconia electrolytes: The influence of two-step sintering profiles on microstructure and gas permeance. International Journal of Applied Ceramic Technologies 2008; 5(6): 589-96. https://doi.org/10.1111/j.1744-7402.2008.02263.x

[4] Ruys AJ, Gingu O, Sima G and Maleksaeedi S. Powder processing of bulk components in manufacturing. In: Nee AYC, Ed. Handbook of Manufacturing Engineering and Technology. London: Springer 2013; 487-566. https://doi.org/10.1007/978-1-4471-4976-7_48-4

[5] Teisanu C and Sima G. Solid state foaming in two steps sintering to produce HAP-based biocomposites for bone grafting. In: Rotaru A, Ed. Advanced Engineering Materials.

Recent Developments for Medical, Technological and Industrial Applications. Rostock: Academica Greifswald Publishing House 2016; 43-86.

[6] Gingu O, Cojocaru D, Ristoscu CG, Sima G, Teisanu C and Mangra M. The influence of the foaming agent on the mechanical properties of the PM hydroxyapatite-based biocomposites processed by two-step sintering route. Journal of Optoelectronics and Advanced Materials 2015; 17(7-8): 1044-49.

[7] Marinescu C, Sofronia A, Anghel EM, Baies R, Constantin D, Seciu AM, et al. Microstructure, stability and biocompatibility of hydroxyapatite-titania nanocomposites formed by two-step sintering process. Arabian Journal of Chemistry 2017; available online: https://doi.org/10.1016/j.arabjc.2017.01.019 https://doi.org/10.1016/j.arabjc.2017.01.019

[8] Pascu CI, Gingu O, Ciupitu I and Rotaru P. Biocomposite material and its elaboration process. Romanian Patent 125714. 2015.

[9] Burstein FD. State of the art: Bone substitutes. Cleft Palate Craniofac J 2000; 37: 1-3 https://doi.org/10.1597/1545-1569(2000)037<0001:ESNTIT>2.3.CO;2

[10] Schnettler R, Stahl JP, Alt V, Pavlidis T, Dingeldein E and Wenisch S. Calcium phosphate-based bone substitutes. Eur J Trauma 2004; 30(4): 219-29. https://doi.org/10.1007/s00068-004-1393-x

[11] Mour M, Das D, Winkler T, Hoenig E, Mielke G, Morlock MM, et al. Advances in porous biomaterials for dental and orthopaedic applications. Materials 2010; 3(5): 2947-74 https://doi.org/10.3390/ma3052947

[12] Dobos P. Synthesis of foamed bioceramics for potential medical applications, M. Ph.D. Thesis, Brno University of Technology, Faculty of Chemistry (2011).

[13] Liu H, He P, Feng JC and Cao J. Kinetic study on nonisothermal dehydrogenation of TiH2 powders. Int J Hydrogen Energy 2009; 34: 3018-25. https://doi.org/10.1016/j.ijhydene.2009.01.095

[14] Blowing agents. Available from: http://www.icodassociates.com/docs/blowing_agents.pdf

[15] Kevorkijan V. Low cost aluminium foams made by CaCO3 particulates. Metall and Mat Eng 2015; 16(3): 205-19.

[16] Halikia I, Zoumpoulakis L, Christodoulou E and Prattis D. Kinetic study of the thermal decomposition of calcium carbonate by isothermal methods of analysis. EJMP and EP 2001; 1(2): 89 -102.

[17] Haeshche M, Lehmhus D, Weise JA, Wichmann M and Magnabosco Mocellin IC. Carbonates as foaming agent in chip-based aluminium foam precursor. J Mater Science and Technology 2010; 26: 845-50. https://doi.org/10.1016/S1005-0302(10)60135-1

[18] Li SH, De Wijn JR, Layrolle P and De Groot K. Synthesis of macroporous hydroxyapatite scaffolds for bone tissue engineering. J Biomed Mater Res 2002; 61: 109-120. https://doi.org/10.1002/jbm.10163

[19] Ishiwata K, Tawara K and Matsushita J. Characterization of Hydroxyapatite Containing of Titanium Hydride Sintered Body by Nano Size Powder, Materials Science Forum 2013; 761: 135-139. https://doi.org/10.4028/www.scientific.net/MSF.761.135

[20] Montufar EB, Gil C, Traykova T, Ginebra MP and Planell J. Foamed beta-tricalcium phosphate scaffolds, Key Eng Mater 2008; 361-363: 323-6. https://doi.org/10.4028/www.scientific.net/KEM.361-363.323

[21] Feng P, Niu M, Gao C, Peng S and Shuai C. A novel two-step sintering for nano-hydroxyapatite scaffolds for bone tissue engineering 2014; Sci Rep; 4; 5599. https://doi.org/10.1038/srep05599

[22] Farzin A, Ahmadian M and Fathi MH. Comparative evaluation of biocompatibility of dense nanostructured and microstructured hydroxyapatite/titania composites, Mat Sci and Eng C 2013: 2251-2257. https://doi.org/10.1016/j.msec.2013.01.053

[23] Gingu O, Pascu CI, Lupu N and Benga GC. Material biocompozit si procedeu de elaborare a acestuia, Romanian patent, 125713/2015 - O.S.I.M. Romania.

[24] Rudenko N and Laptev A. Compaction and properties of highly porous powder parts produced with various pore formers. Mechanical Testing and Diagnosis 2001; 1: 82-87.

DOI: http://dx.doi.org/10.15377/2409-5826.2017.04.3

© 2017 Gingu, *et al.*; Avanti Publishers.
This is an open access article licensed under the terms of the Creative Commons Attribution Non-Commercial License (http://creativecommons.org/licenses/by-nc/3.0/) which permits unrestricted, non-commercial use, distribution and reproduction in any medium, provided the work is properly cited.